International Journal of Solids and Structures 80 (2016) 128–136

Contents lists available at ScienceDirect

International Journal of Solids and Structures

journal homepage: www.elsevier.com/locate/ijsolstr

A methodology for obtaining plasticity characteristics of metallic coatings via instrumented indentation

J.L. Reed [a], J. Dean [a,b], G. Aldrich-Smith [c], T.W. Clyne [a,*]

[a] Department of Materials Science and Metallurgy, University of Cambridge, 27 Charles Babbage Road, Cambridge CB3 0FS, UK
[b] Double Precision Consultancy, Salisbury House, Station Road, Cambridge CB1 2LA, UK
[c] AWE, Aldermaston, Reading, Berkshire, RG7 4PR, UK

ARTICLE INFO

Article history:
Received 7 April 2015
Revised 11 September 2015
Available online 6 November 2015

Keywords:
Indentation
Finite element analysis
Coatings
Plasticity

ABSTRACT

A methodology is presented for inferring the yield stress and work-hardening characteristics of metallic coatings from indentation data. It involves iterative use of FEM modelling, with predicted outcomes (load–displacement relationships and residual indent shapes) being systematically compared with experimental data. The cases being considered are ones in which the indenter penetration depth is a significant fraction of the coating thickness, so that the properties of the substrate, and possibly of the interface, are of significance. The methodology is thus suitable for the testing of thin coatings. In the present work, the coatings were in fact relatively thick (hundreds of microns) and the (spherical) indenter penetration was a substantial fraction of this. In this way, the basic validity of the methodology could be investigated with minimal complications from effects related to microstructure, oxide films, surface roughness etc. Furthermore, the properties of both coating and substrate (in the through-thickness direction) were established separately via conventional compression testing. The systems studied were copper (yield stress ~15 MPa) on stainless steel (yield stress ~350 MPa) and vice versa. Both exhibited significant work hardening. It is concluded that the methodology is basically reliable, with relatively good sensitivity and resolution, although this does depend on several factors, which are highlighted in the paper. It is unlikely to be suitable for very thin (sub-micron) films, but should be reasonably accurate for coatings of thickness down to a few microns.

1. Introduction

Instrumented indentation is routinely used for obtaining Young's moduli of materials from the load–displacement curve during unloading (elastic recovery). The procedure is also applied to coatings. If the penetration depth of the indenter is small compared with the coating thickness, then this situation is no different from that with a bulk sample. There is, however, the issue of how "small" should be defined in this context. A "rule of thumb" figure of 10% is often used, although there is no clear theoretical basis for this and it seems likely that the ratio of Young's moduli of coating and substrate will affect the outcome. The most straightforward approach, proposed by Jennett and Bushby (Jennett and Bushby, 2001), involves indenting to a range of depths and obtaining the 'combined' modulus of coating and substrate, as a function of the ratio of the penetration depth to the coating thickness, h/t. The value of E for the coating is then found by extrapolating back to $h/t = 0$. Since there is no well-defined functional form for the extrapolation, at least some measured moduli are needed for relatively low h/t values: obtaining reliable values for these, particularly with thin coatings, is, of course, the central problem. Nevertheless, the approach is clearly preferable to solely relying on data from one or two very shallow indents.

Various analyses and methodologies taking account of the presence of the substrate have been developed. For example, Doerner and Nix (Doerner et al., 1986) included a term for the substrate in their reduced Young's modulus equation. However, the scaling constants used are only appropriate for specific cases. King (King, 1987) presented a modified solution, using FEM, to arrive at an equation for the reduced Young's modulus, later validated by Saha and Nix (Saha and Nix, 2002). Gao et al (Gao et al., 1992) used a moduli perturbation method to develop a closed-form solution for the reduced Young's modulus of a coating, later shown to be inaccurate when the mismatch between Young's moduli of coating and substrate is large (Chen and Vlassak, 2001). Xu and Pharr (Xu and Pharr, 2006) suggested a modification to make it more accurate, verified using FEM. Investigations have also been made (Tricoteaux et al., 2010) into the effect of machine compliance in this context. In general, it is possible, using such approaches, to obtain a reasonably reliable value for the stiffness of a coating via indentation.

* Corresponding author. Tel.: +44 1223 334332; fax: +441223334567.
E-mail address: twc10@cam.ac.uk (T.W. Clyne).

http://dx.doi.org/10.1016/j.ijsolstr.2015.10.029
0020-7683/

However, the problem is clearly more complex when plasticity (and/or creep) is involved. Of course, this also presents much greater challenges for bulk samples than does stiffness. This statement does not really apply to hardness, which is defined in terms of an indentation response. However, hardness is not a fundamental or well-defined material property, since it depends, not only on yield stress and work hardening characteristics, but also on indenter shape and in some cases on indentation depth. While there has been a lot of work on the measurement of hardness for thin surface coatings, it is therefore excluded from the current discussion.

The difficulty in obtaining plasticity and creep characteristics from indentation experiments arises from the complex and continuously changing stress and strain fields under the indenter. As a consequence of this, while there have been many attempts to identify methodologies involving the use of analytical equations for evaluation of these characteristics from indentation data, it now seems clear that none of them are consistently reliable. Reliable inference of these characteristics requires these fields to be taken into account in a quantitative manner. The most suitable tool for this is the finite element method (FEM), which has been widely applied to indentation testing with the objective of obtaining information about plasticity parameters (Bouzakis and Vidakis, 1999, Bouzakis et al., 2001, Tunvisut et al., 2001, Liu et al., 2005, Pelletier, 2006, Yonezu et al., 2009, Pohl et al., 2014). In particular, a consistent methodology, based on iterative use of FEM, has recently been developed that allows the yield stress and work hardening rate (Dean et al., 2010) and the (primary and secondary) creep parameters (Dean et al., 2013) to be inferred from experimental indentation data. These capabilities, for which customised user-friendly software packages are currently being prepared, would be further enhanced if the methodology could be extended to (relatively thin) coatings, for which the effect of the substrate on the indentation response cannot be ignored (i.e. cases for which the penetration depth is not "small" relative to the coating thickness).

There have also been various attempts to establish the maximum h/t ratio for which it is acceptable to treat a coating as a bulk material for evaluation of plasticity parameters (Lebouvier et al., 1985, Sun et al., 1995, Panich and Sun, 2004, Gamonpilas and Busso, 2004) (and hardness (Cai and Bangert, 1995, Xu and Rowcliffe, 2004)). In general, values of around 10% are often quoted, although it is clear that there is considerable scope (Chudoba et al., 2002, Cleymand et al., 2005) for variations in this figure (more so for plasticity than for Young's modulus) between different systems, which is unsurprising in view of the larger number of material properties (for coating and substrate) expected to be relevant. It appears that no rationale has been developed so far that has led to a reliable analytical expression for this "critical ratio".

In the present work, a methodology is presented for extraction of plasticity parameters (including work hardening characteristics) of coatings from indentation data, applicable for any ratio of indentation depth to coating thickness (irrespective of coating and substrate properties). A spherical indenter has been used. Of course, unlike a Vickers or a Berkovich, or indeed a cone, this shape is not self-similar, which has implications for the development of the strain field. It might be argued that the changing strain field encompasses a wider range of conditions for a shape that is not self-similar, and that this is beneficial. Of course, a sphere is also transversely isotropic (as indeed is a cone), which allows a 2-D model to be employed (provided the sample is also transversely isotropic). In practice, it might be advantageous (in terms of converging rapidly to a unique solution) to employ at least two different indenter shapes in the same study. Nevertheless, in the present work only a spherical indenter has been employed.

An important point in the context of the current study concerns effects of scale. The work involves use of very coarse (thick) coatings (and large indenters). This is done so as to allow use of coating materials for which the properties (in the direction of indentation) can be obtained by conventional testing. The mechanical modelling (and indeed, at least in principle, the actual behaviour) is scale-independent – so that, for example, the stress and strain field around a spherical indenter that has penetrated a (bulk) sample to 10% of its radius is the same whether that radius is 10 μm or 10 mm. This allows universal deductions to be made from experiments carried out on a very coarse scale. In practice, scale effects may arise if the characteristic length scales of the testing become comparable to those relevant to the micro-mechanisms of deformation, such as the distances between dislocations or the grain size. However, the current work is focused on the extraction of "continuum" (macroscopic, or bulk) properties and these should, of course, be scale-independent.

2. Experimental procedures

2.1. Materials and microstructures

Two materials were used – an oxygen-free, high conductivity (OFHC) copper and an austenitic stainless steel (AISI 304). The steel microstructure is shown in Fig. 1(a), demonstrating that the grain size is ~30–50 μm. The copper, received in extruded rod form, was annealed inside vacuum-sealed ampoules for 2 h at 800°C, to stimulate recrystallisation and reduce the hardness. The resulting grain structure is shown in Fig. 1(b), where it can be seen that the grain size is ~100 μm. (These grain sizes are sufficiently coarse to create difficulties in ensuring multi-grain interrogation during conventional nanoindentation, but in the present work the indent diameters were of the order of at least several hundred microns.)

2.2. Macroscopic, uniaxial compression testing

In many systems, particularly for thin coatings, mechanical properties in the through-thickness direction (normal to the free surface) are largely unknown. However, it is these properties that dominate the indentation response and so it was important to obtain them for validation of the methodology. Specimens for uniaxial compression testing were machined from the as-received stainless steel and the annealed copper rod. Cylindrical specimens (12 mm in height and 10 mm in diameter) were tested in compression, at room temperature, using a 100 kN ESH servo-hydraulic mechanical test machine. The ends were lubricated with molybdenum disulphide, to minimise barrelling. Displacements were measured using a scanning laser system, with a resolution of ~3 μm.

2.3. Soft (copper) coatings on a hard (steel) substrate

Thin discs of Cu (300 μm thick) were machined (sliced) from extruded rods by electro-discharge machining (EDM). Some of these were polished down, to generate discs about 165 μm thick. Both types of disc were attached to stainless steel substrates, using a high-strength Araldite adhesive. In order to minimise the thickness of the adhesive layer, it was first heated over a hot-plate. The consequent reduction in viscosity allowed a thin, continuous layer (~10 μm thick) to form. It was cured for 24 h at room temperature.

Samples were indented using a custom-built, screw-driven mechanical test machine, with a load capacity of 2.5 kN. The indenter was a commercially-available 3 mm diameter sphere of tungsten carbide (a WC cermet). The indenter was therefore very large, at least in comparison to more conventional micro- and nanoindenters, giving benefits in terms of sampling a representative volume, being immune to errors associated with oxide films, surface roughness etc., and creating depth data with excellent relative accuracy. (Outcomes

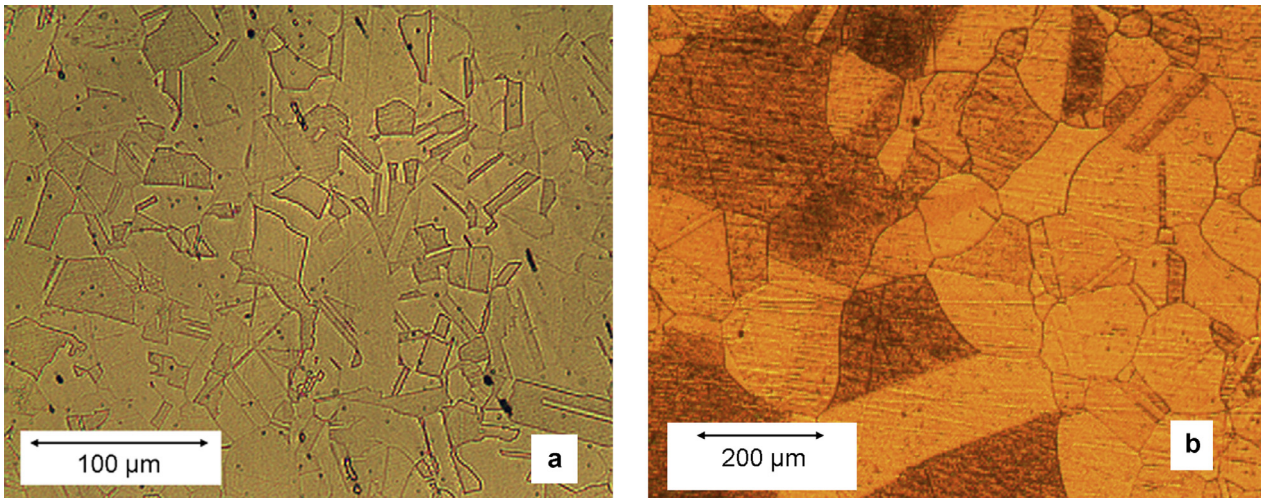

Fig. 1. Optical micrographs showing the grain structures of (a) 304 stainless steel and (b) OFHC copper.

from these procedures should thus be scale-independent.) The indenter load was increased to a prescribed value at a displacement rate of 1.66 μm s^{-1} (sufficiently fast for creep deformation to be negligible with this system), and then reduced at the same rate.

Some measurements were also made of residual indent shapes, using a Dektak profilometer. This was done for all 4 cases (bulk Cu, bulk steel and the two thicknesses of Cu on steel), using a 2 mm diameter WC indenter. (The smaller indenter was used for this work in order to ensure that the depths were within the range of the profilometer.) Residual indent depths were measured relative to the far field level of the specimen surface. This procedure was repeated several times, at different locations on the specimen surface, and with different applied peak loads.

2.4. Hard (steel) coating on a soft (copper) substrate

Discs of steel (2 mm thick) were machined (sliced) from extruded rods by electro-discharge machining (EDM). These were attached to Cu substrates using an adhesive, as in §2.3. Samples were indented using a 25 kN Tinius Olsen mechanical testing machine. The indenter was again a 3 mm diameter sphere of WC. The indenter load was increased to a prescribed value at a displacement rate of 1.66 μm s^{-1} and reduced at the same rate. Load–displacement curves were obtained and compliance corrections applied. This process was repeated several times, at different locations on the specimen surface.

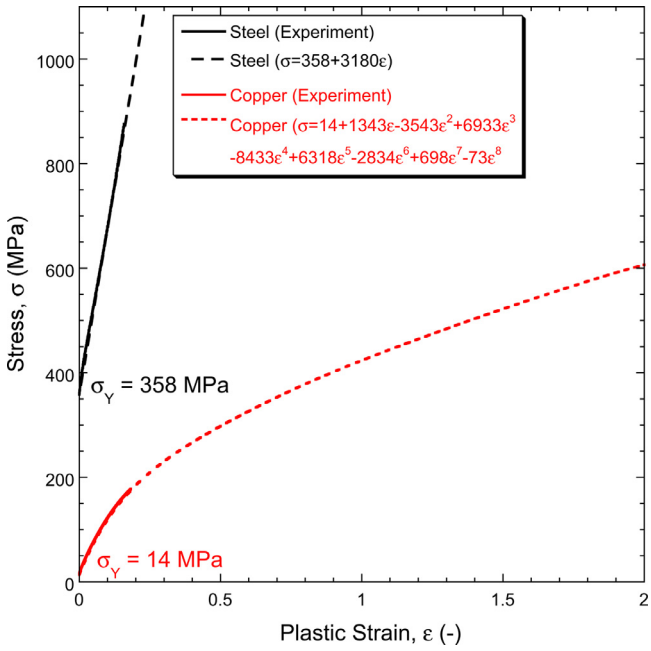

Fig. 2. Stress–strain curves, measured in compression, for the steel and the copper, together with modelled curves (and showing the equations employed to produce them).

3. Finite element modelling

3.1. Geometry, meshing and mechanical boundary conditions

Axi-symmetric FEM models were built using ABAQUS/CAE. The indenters were modelled as analytical rigid bodies. Coating and substrate materials were modelled as deformable bodies and meshed with linear quadrilateral (hybrid) elements. (Hybrid element formulation is recommended for incompressible materials and when deformation is dominated by plastic flow.) Meshes were refined in regions close to the indenter. Sensitivity analyses confirmed that the meshes were sufficiently fine to achieve convergence, numerical stability and mesh-independent results. Fixed loads were prescribed as boundary conditions at the indenter. The indenter displacement history was an output (solution) from the model, for comparison with experimental data. Coatings and substrates were taken to be bonded at the interface and the adhesive layer was neglected. When predicting residual indent shapes (including depths), the effect of elastic recovery during unloading was taken into account.

3.2. Constitutive material behaviour

Young's moduli of 122 and 210 GPa (isotropic) were used for the copper and steel, respectively. (These values were very close to those obtained from the initial unloading sections of the indentation data.) Yield stresses and work-hardening characteristics were also taken as isotropic and values obtained experimentally were used to characterise plasticity in the models. (It may be that these materials were not plastically isotropic, but the behaviour during indentation is expected to be dominated by the values in the through-thickness direction – i.e. those that were measured.) For the copper, the yield stress was 14 MPa, whereas that of the steel was 358 MPa. Measured stress versus plastic strain curves for the two materials are shown in Fig. 2, together with analytical curves used in the model (extrapolated to the maximum levels of strain created in the indentation simulations). It can be seen that these curves reflect the experimental data quite closely, although it is, of course, difficult to obtain experimental information for uniaxial loading at very high plastic strains (either in tension, because of plastic instability, or in compression, because of

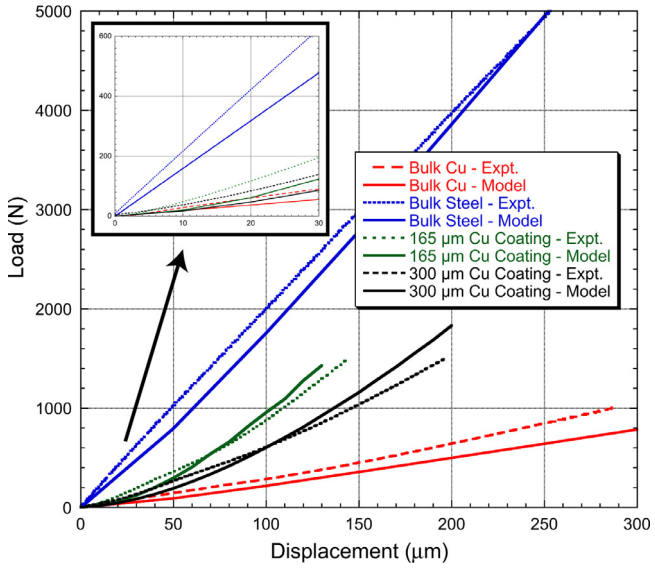

Fig. 3. Measured and predicted load–displacement data, for indentation of bulk steel, bulk Cu and for two thicknesses of Cu on steel, using a 3 mm diameter WC sphere.

barrelling). During indentation of a coating, on the other hand, particularly for a soft coating on a harder substrate, and for penetration to a significant proportion of the coating thickness, the plastic strains can become very large. Hence this extrapolation is unavoidable.

4. Indentation of bulk copper and steel specimens

Measured load–displacement data are presented in Fig. 3 for the two bulk materials. Predicted plots are also shown, obtained using the (von Mises) stress–strain relationships shown in Fig. 2. It can be seen that there is good agreement for both materials.

5. Indentation of soft (copper) coatings on hard (steel) substrates

5.1. Load–displacement curves

Also shown in Fig. 3 are experimental and predicted load–displacement data for the two coating thicknesses, obtained using the (von Mises) stress–strain relationships shown in Fig. 2. It can be seen that the loads for the coatings start to rise above that for the bulk Cu almost immediately, corresponding to depth/coating thickness ratios well below 10%. This suggests that the "rule of thumb" that the presence of the substrate can be ignored for indentation depths $<\sim$10% of the coating thickness is not reliable for this case (i.e .for soft coatings).

The experimental behaviour for the coatings is captured well by the model, including the gently increasing gradient of the plots. This gradient increase is caused by greater constraint on coating deformation as the indenter approaches the substrate, raising the local coating strains (see §5.3), such that the work (strain) hardening effect becomes substantial. The observed level of agreement confirms the reliability of the model, the incorporated assumptions (including perfect interfacial bonding) and the measured material property data. Of course, for the materials used here, the substrate hardness is much greater than that of the coating – indeed, the substrate remains elastic during these experiments (see §5.3). It is also worth noting that the Cu has a relatively high work hardening rate, so its flow stress in the plastic strain range of interest is well above the yield stress.

5.2. Residual indent shapes

Predicted residual indent shapes are compared to measured Dektak profilometer traces in Fig. 4. The measured data comprise 4 scans, taken at 0°, 45°, 90° and 135°, with the scan length extending across the indent into regions that were nominally flat. It can be seen in Fig. 4(a) that the degree of "pile-up" in the bulk Cu is both predicted and observed to be rather limited. In fact, the experimental curves appear to exhibit some "sink-in". For the bulk steel, on the other hand (Fig. 4(b)), a marked degree of pile-up is both predicted and observed. This is consistent with the plastic strains being appreciably smaller with the steel, which has both a higher yield stress and a higher work hardening rate than the Cu. In general, the model captures the behaviour well in both cases (for residual indent shapes, as well as for the load–displacement behaviour).

As can be seen in Fig. 4(c) and Fig. 4(d), however, there is considerable pile-up formation for the Cu coatings, particularly for the thinner coating (Fig. 4(c)). The steel substrate remains approximately elastic, so the Cu is forced to undergo large plastic strains in the region immediately beneath the indenter, particularly for the thinner coating. This leads to substantial quantities of Cu being forced into the pile-up region, with the (harder) substrate inhibiting sink-in. The level of agreement between model and experiment is not very close for these coatings, particularly for the thinner one. These differences may be at least partly attributable to errors in the modelled extrapolation of the stress–strain curve well beyond the plastic strain range that was measurable experimentally. It is also possible that the assumption of perfect bonding at the interface becomes unreliable when very high plastic strains are created in its vicinity.

5.3. Plastic strain fields

It is clearly important to take into account the nature of the plastic strain fields within the coating and to appreciate the differences compared with corresponding bulk material. Predicted plastic strain fields are shown for two such cases in Fig. 5, both relating to an indentation depth of 250 μm and an indentation sphere of diameter 2 mm. Fig. 5(a) is for bulk Cu, while Fig. 5(b) refers to a 300 μm thick Cu coating on a steel substrate. It is clear that the plastic strains in the Cu are considerably higher in the coating (when the penetration depth is not small compared with the coating thickness) than they are in the bulk. The peak values in the case shown, for example, are $\sim$80% in the bulk and $\sim$180% in the coating. Clearly, the difference between these values will increase sharply as the ratio of penetration depth to coating thickness starts to approach 100%. Again, these predictions are based on the assumption of perfect interfacial bonding and it is possible that in some systems interfacial debonding and sliding could occur. This could change the indentation response significantly. It can also be seen in Fig. 5(b) that there is no plastic strain in the substrate.

It is also worth noting that very high levels of plasticity, while they can be handled within a suitable FEM model, may become unsustainable in practice. In many situations, particularly with significant rates of work hardening, there would be a limit on the ductility, beyond which some kind of damage (such as extensive microcracking or macroscopic fracture) would start to occur. The stress field under an indenter, for a deeply penetrated, soft coating, admittedly incorporates a compressive hydrostatic component, and there is a high level of triaxial constraint, but nevertheless some sort of (irreversible) damage might eventually be expected to arise (Martinez-Gonzalez et al., 2015, Ghosh and Prakash, 2013). Clearly this would make interpretation of indentation data very difficult.

5.4. Sensitivity of indentation load to yield stress and work hardening rate

If the yield stress and work hardening characteristics are to be inferred from experimental indentation curves, then the sensitivities involved are important, since they are likely to dictate the reliability and accuracy of the inferred values. These sensitivities can be

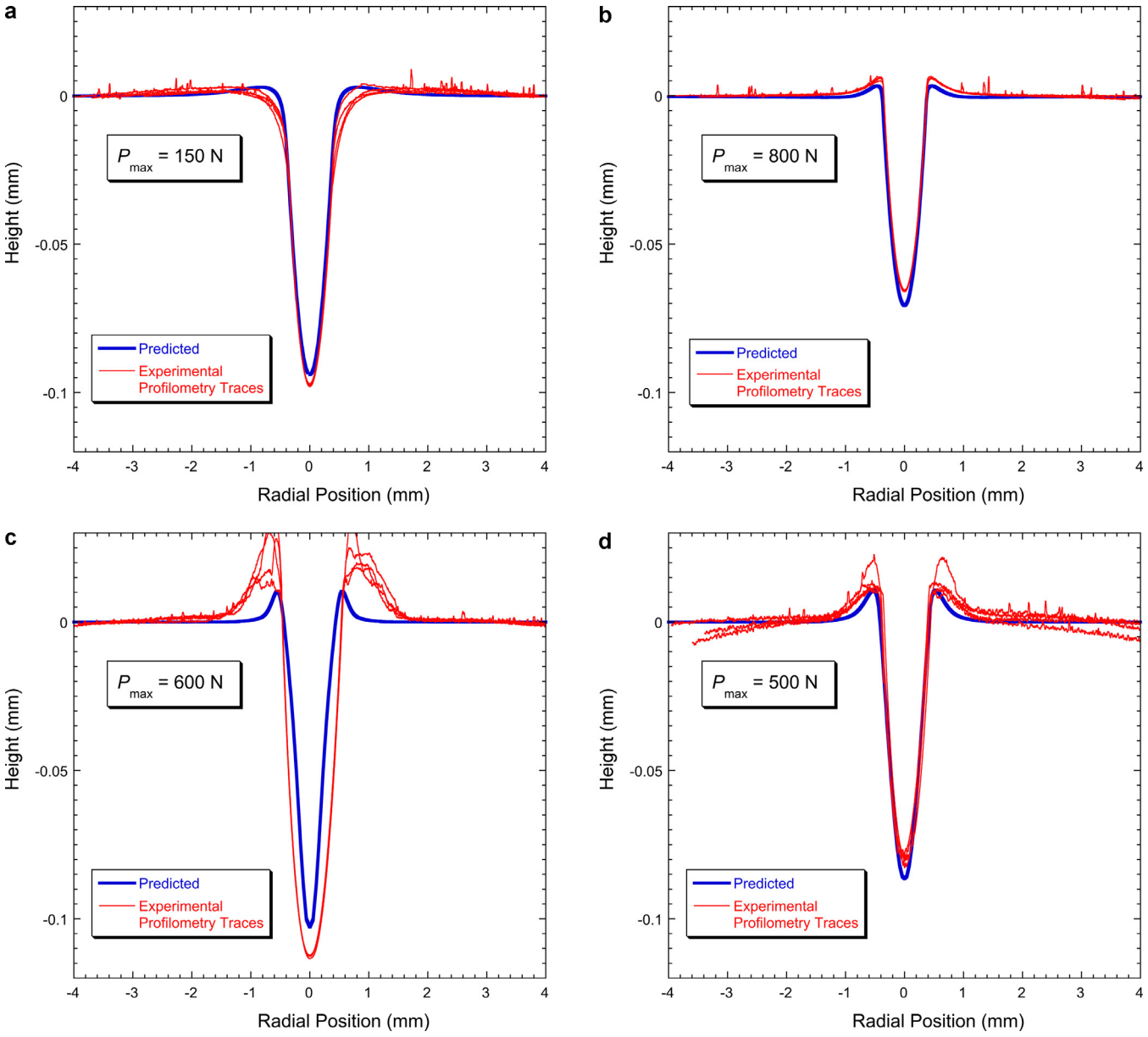

Fig. 4. Measured and predicted residual indent shapes for (a) bulk Cu, loaded to 150 N, (b) bulk steel, loaded to 800 N, (c) Cu coating (165 μm thick) on steel, loaded to 600 N, and (d) Cu coating (300 μm thick) on steel, loaded to 500 N. The indenter was a 2 mm diameter WC sphere.

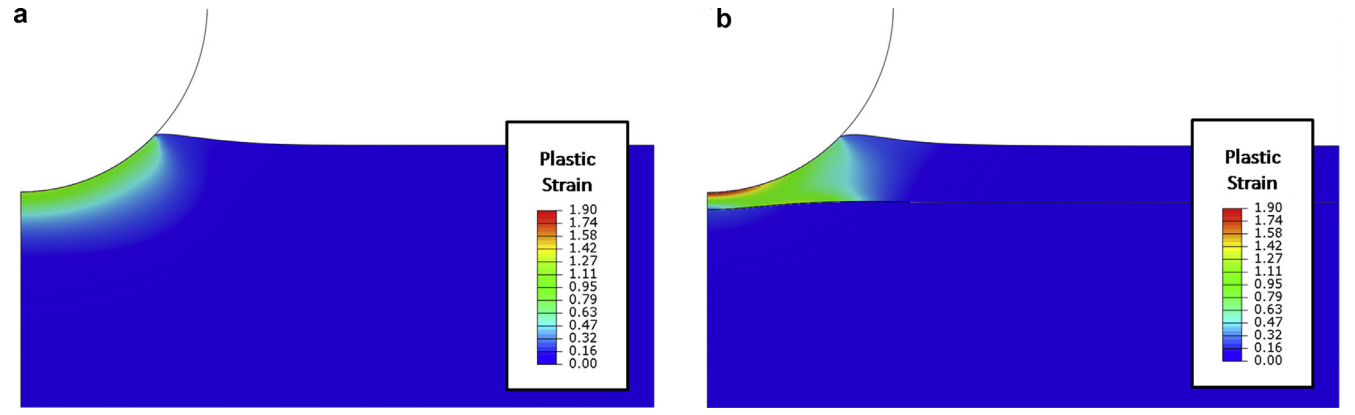

Fig. 5. Predicted equivalent plastic strain fields for indentation (with a rigid 2 mm diameter sphere) of (a) bulk Cu and (b) a 300 μm thick Cu coating on a steel substrate. Both indents are to a depth of 250 μm.

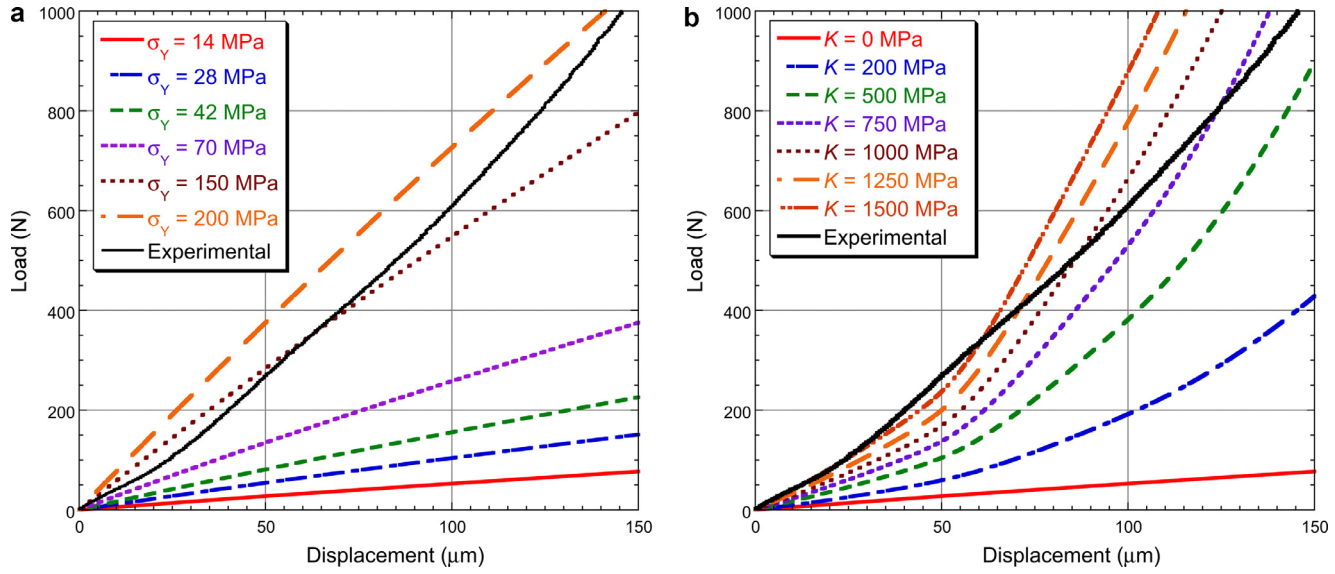

Fig. 6. Comparison between experimental and modelled load–displacement data, for indentation of a 300 μm Cu coating on a steel substrate, using a 3 mm diameter WC sphere, showing the effects of: (a) coating yield stress, with no work hardening, and (b) coating work hardening rate, K (assumed constant), with a yield stress of 14 MPa.

explored by running the FEM model with different input values. The sensitivity to properties of the Cu is illustrated in Fig. 6, for a 300 μm thick Cu coating (with a linear work hardening rate, K), indented with a 3 mm diameter sphere. In Fig. 6(a), the effect of changes in yield stress is shown (for zero work hardening). The actual yield stress of the Cu was 14 MPa (Fig. 2), but it can be seen that, in the absence of work hardening ($K = 0$), the model gives predictions that could lead to a highly inaccurate value of the yield stress (~150 MPa) being inferred. It is clear that, at least in this case (with the flow stress at substantial plastic strains being much greater than the yield stress), work hardening must be taken into account.

The sensitivity to the work hardening rate, K (assumed constant) is illustrated in Fig. 6(b), in which the yield stress is given its correct value (14 MPa). There are some noteworthy features. For instance, if the Cu is assumed to exhibit no work hardening, then the loads are massively under-predicted (see above). The inferred value of K would probably be ~700–1000 MPa, although this might depend on the depth to which indentation was taken. The plot in Fig. 2 indicates that the correct value of K (gradient of the plot) is initially ~1000 MPa, although it falls to ~15–20 MPa at large strains (admittedly in a regime in which it has had to be highly extrapolated). Of course, these large changes in K with increasing plastic strain explain why the experimental data do not agree well with any of the modelled curves in Fig. 6(b). Clearly, in this particular case, it would be necessary to try different functional forms for the work hardening curve, as well as different values for the parameters, if good agreement is to be obtained. Of course, the level of agreement shown in Figs. 3 and 4 does indicate that such convergence is possible and the plots in Fig. 6(b) would probably have provided sufficient warning that the coating did not exhibit linear work hardening. The indent shape comparisons provide extra degrees of freedom for optimising convergence.

6. Indentation of hard (steel) coatings on soft (copper) substrates

6.1. Load–displacement curves

Fig. 7 shows experimental and predicted load–displacement curves, with modelled plots obtained using the (von Mises) stress–strain relationships shown in Fig. 2. In this case, the load for the coating starts to fall below that for the bulk steel at displacements above about 40 μm, representing a depth/coating thickness ratio of ~2%. This again raises concerns about the "10% rule of thumb".

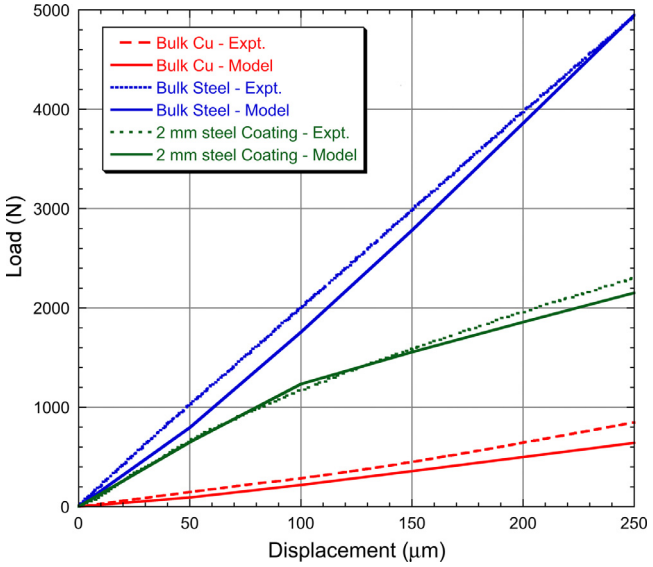

Fig. 7. Measured and predicted load–displacement data, for indentation of bulk steel, bulk Cu and a 2 mm thick steel coating on Cu, using a 3 mm diameter WC sphere.

The experimental behaviour is again captured well by the model. The gradient reduction with increasing penetration (particularly after about 100 μm penetration) arises from progressive plastic deformation of the substrate (which was negligible for the Cu-on-steel cases). If a thinner steel coating had been used, the onset of this would have taken place earlier. In fact, if the coating thickness had been similar to the Cu-on-steel cases, then it would have started immediately. The observed level of agreement confirms the reliability of the model, the incorporated assumptions (including perfect interfacial bonding) and the measured material property data.

6.2. Plastic strain fields

The plastic strain fields are again helpful in understanding deviations from bulk behaviour. A predicted plastic strain field is shown in Fig. 8, for 250 μm penetration into a 2 mm thick steel coating on Cu. Even for this depth (~12% of the coating thickness) there is

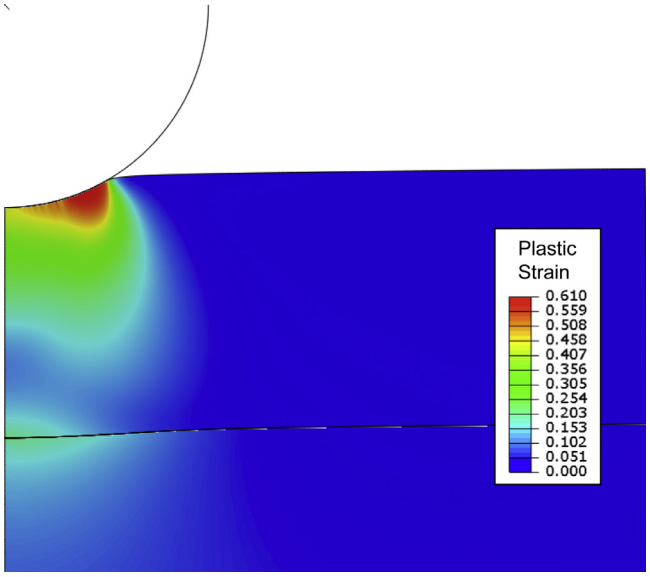

Fig. 8. Predicted equivalent plastic strain field for indentation (with a rigid 3 mm diameter sphere) of a 2 mm thick steel coating on a Cu substrate to a depth of 250 μm.

considerable plasticity in the Cu substrate - the peak plastic strain in the coating is ~60%, while that in the substrate is ~30%. Such substrate plasticity will strongly influence load–displacement curves, even when the ratio of penetration depth to coating thickness is small.

6.3. Sensitivity of indentation load to yield stress and work hardening rate

Again, the sensitivities are important if yield stress and work hardening characteristics are to be inferred from experimental indentation curves. These can be explored via model predictions. The sensitivity to properties of the steel is illustrated in Fig. 9, for a 2 mm thick steel coating (with linear work hardening). In Fig. 9(a), the effect of changes in yield stress is shown (with the correct work-hardening rate (3000 MPa, assumed constant)). It can be seen that the outcome is quite sensitive to the yield stress and an approximately correct value (~350 MPa) would probably be deduced.

The sensitivity to work hardening rate (assumed constant) is illustrated in Fig. 9(b), in which the yield stress is taken to have its correct value (358 MPa). The predictions are less sensitive to changes in K than was the case for the Cu coating (in which larger plastic strains were created). It can be seen that the value of K that would be inferred is ~3000–6000 MPa – i.e. an accurate value might be difficult to obtain, although it is of the correct order of magnitude. In this case, of course, the coating does have an approximately constant work hardening rate, and the coating strains are relatively low, so the uncertainties of the Cu-on-steel case are largely avoided.

It is also clear, however, that the model predictions will be sensitive to the plasticity parameters of the substrate, which was not the case for Cu-on-steel. The sensitivity of the predictions to the properties of the Cu is illustrated in Fig. 10. The coating properties were fixed at the correct values (358 MPa and 3000 MPa). Fig. 10(a) shows the effect of changes in substrate yield stress (with no work-hardening). The predictions are sensitive to changes in the yield stress even at low indent depths. Again, neglect of work hardening makes the predictions very inaccurate.

The sensitivity to substrate work hardening rate (assumed constant) is illustrated in Fig. 10(b), with the yield stress given its correct value (14 MPa). Again, it can be noted that, in the absence of work hardening in the substrate, the predicted loads are under-predicted. It can be seen that a K value of ~750 MPa would correctly predict the response: in this case, since the strains in the Cu substrate are relatively small (<~30%), a constant value of K of this magnitude is a reasonably good representation of the behaviour – see Fig. 2. Of course, in practice it is usually straightforward to obtain accurate substrate plasticity properties. These examples illustrate the importance of doing this for cases in which plastic deformation of the substrate is significant.

Of course, it should be recognised that there has been no systematic convergence on "correct" solutions in the present work, or checking of their uniqueness. Algorithms for this, preferably implemented within customised software packages, will need to be developed (Dean et al., 2010) for bulk samples before they can be considered for coatings. This will certainly require systematic exploration of parameter space, and use of multiple experimental outcomes (e.g. using different indenter shapes), if inferred property values are to be reasonably accurate and reliable. Nevertheless, such packages will be possible for coatings and factors identified in the present paper should be useful for this development.

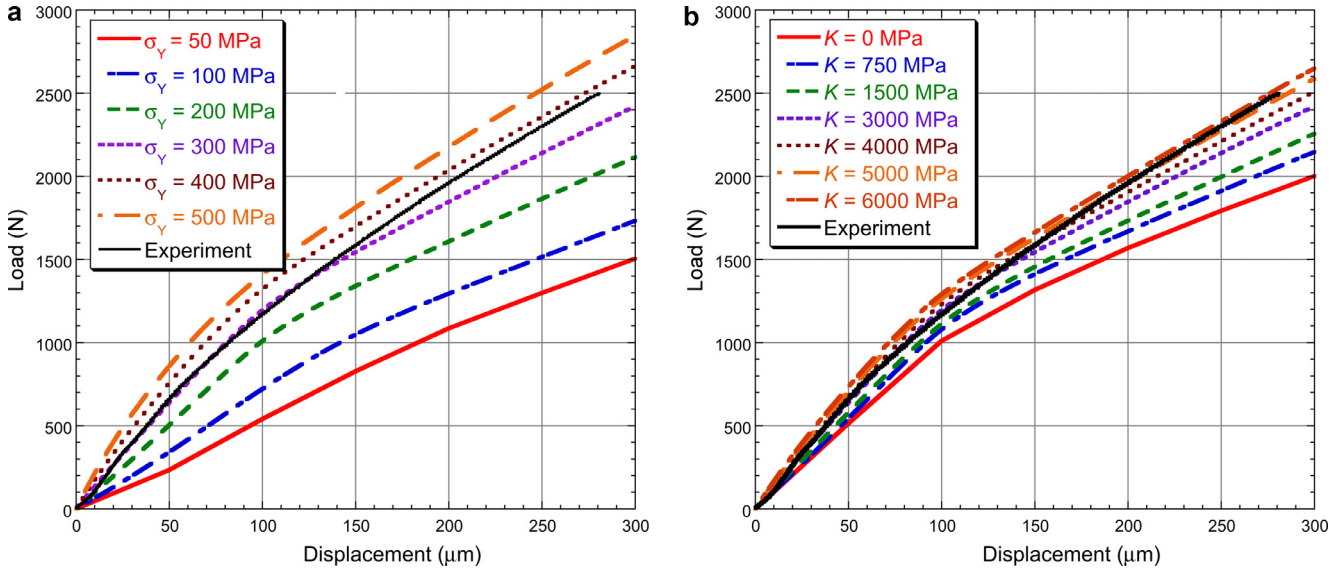

Fig. 9. Comparison between experimental and modelled load–displacement data, for indentation of a 2 mm steel coating on a Cu substrate, using a 3 mm diameter WC sphere, showing the effects of: (a) coating yield stress, with a (constant) work hardening rate of 3000 MPa, and (b) coating work hardening rate, K (constant), with a yield stress of 358 MPa.

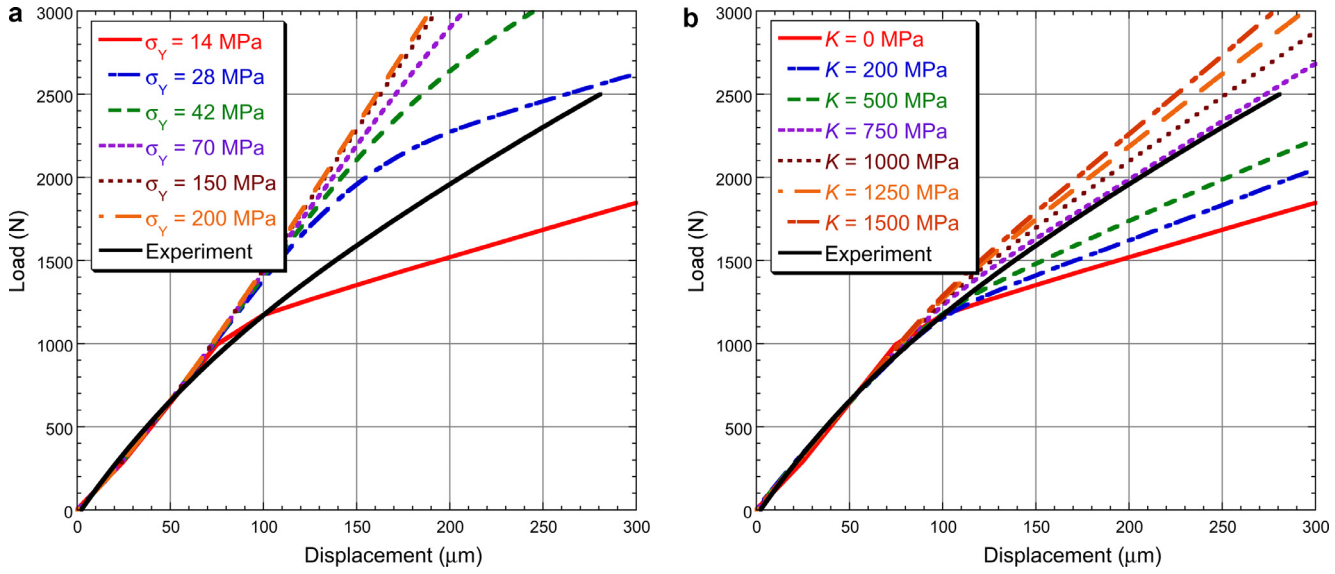

Fig. 10. Comparison between experimental and modelled load–displacement data, for indentation of a 2 mm steel coating on a Cu substrate, using a 3 mm diameter WC sphere, showing the effects of: (a) substrate yield stress, with no work hardening, and (b) substrate work hardening rate, K (constant), with a yield stress of 14 MPa.

7. Conclusions

The following conclusions can be drawn from this work, which is aimed at obtaining plasticity parameters of coatings from indentation to a significant fraction of their thickness. By using thick coatings (hundreds of microns) and deep penetration, various complications and uncertainties have been avoided. It has also enabled experiments to be carried out using "coatings" with known properties in the through-thickness direction.

(a) FEM modelling has been used to simulate indentation. Input data included the (von Mises) stress–strain relationships for the two materials, with no time dependence. Conclusions have been drawn about the reliability of yielding and work hardening parameters obtained by iterative optimisation of agreement between modelled and experimental indentation responses. In general, this methodology is shown to be viable for obtaining the plasticity parameters of (metallic) coatings (penetrated to a significant fraction of their thickness).

(b) For soft coatings on hard substrates, large plastic strains are generated in the coating under the indenter, whereas the substrate is likely to remain elastic or experience only small plastic strains. The response is thus sensitive to the work hardening rate of the coating (unless it is very low) and to its variation with strain. For the materials employed, it would have been possible to infer both the yield stress and the work hardening characteristics of the coating quite accurately, although the latter has to be represented via some appropriate (non-linear) function. This introduces extra degrees of freedom and hence a requirement for more comprehensive comparisons between experimental data and model predictions.

(c) For hard coatings on soft substrates, significant plasticity is likely in the substrate. Of course, substrate properties will often be easy to obtain. The sensitivity of the indentation response to the plasticity parameters of the coating is likely to be reduced by this dependence on substrate properties. On the other hand, since plastic strains in the coating will be relatively small, an assumption of linear work hardening may be acceptable, simplifying the analysis.

(d) For both types of system, it is both predicted and observed that the indentation response of a coating starts to deviate from that of the corresponding bulk material at very low ratios of indentation depth to coating thickness – well below the 10% figure that is often quoted as being acceptable for neglect of the presence of the substrate.

(e) It is felt that the methodology is viable and could be used to infer coating properties solely from indentation data, via appropriate FEM modelling. The information presented here concerning sensitivities etc. may be helpful during implementation. This procedure is always likely to be difficult for very thin coatings, but may be practicable for thicknesses down to a few microns.

Acknowledgements

This work has been supported by EPSRC (grant RG62695) and also by AWE, as part of an ongoing collaboration aimed at the development of robust and user-friendly tools for the extraction of mechanical property characteristics from instrumented indentation data.

In compliance with current EPSRC requirements, the input data for the indentation modelling described in this paper, including meshing and boundary condition specifications, are available at the following URL: www.ccg.msm.cam.ac.uk/publications/resources. These files can be downloaded and used in ABAQUS FEM models. Data supplied are for a representative case (with a spherical indenter and radial symmetry).

References

Bouzakis, K.D., Michailidis, N., Erkens, G., 2001. Thin hard coatings stress-strain curve determination through a FEM supported evaluation of nanoindentation test results. Surf.Coat. Techn. 142, 102–109.

Bouzakis, K.D., Vidakis, N., 1999. Superficial plastic response determination of hard isotropic materials using ball indentations and a FEM optimization technique. Mater. Charact. 42, 1–12.

Cai, X., Bangert, H., 1995. Hardness measurements of thin films - determining the critical ratio of depth to thickness using FEM. Thin Sol. Films 264, 59–71.

Chen, X.M., Vlassak, J.J., 2001. Numerical study on the measurement of thin film mechanical properties by means of nanoindentation. J. Mater. Res. 16, 2974–2982.

Chudoba, T., Schwarzer, N., Richter, F., 2002. Steps towards a mechanical modeling of layered systems. Surf. Coat. Technol. 154 (2–3), 140–151.

Cleymand, F., Ferry, O., Kouitat, R., Billard, A., von Stebut, J., 2005. Influence of indentation depth on the determination of the apparent young's modulus of bi-layer material: experiments and numerical simulation. Surf. Coat. Technol. 200 (1-4), 890–893.

Dean, J., Bradbury, A., Aldrich-Smith, G., Clyne, T.W., 2013. A procedure for extracting primary and secondary creep parameters from nanoindentation data. Mech. Mater. 65, 124–134.

Dean, J., Wheeler, J.M., Clyne, T.W., 2010. Use of quasi-static nanoindentation data to obtain stress-strain characteristics for metallic materials. Acta Materialia 58, 3613–3623.
Doerner, M.F., Gardner, D.S., Nix, W.D., 1986. Plastic properties of thin films on substrates as measured by submicron indentation hardness and substrate curvature techniques. J. Mater. Res. 1, 845–851.
Gamonpilas, C., Busso, E.P., 2004. On the effect of substrate properties on the indentation behaviour of coated systems. Mater. Sci. Eng. A 380, 52–61.
Gao, H.J., Chiu, C.H., Lee, J., 1992. Elastic contact versus indentation modeling of multilayered materials. Int. J. Sol. Struct. 29 (20), 2471–2492.
Ghosh, S., Prakash, R.V., 2013. Study of damage and fracture toughness due to influence of creep and fatigue of commercially pure copper by monotonic and cyclic indentation. Metall. Mater. Trans. A-Phys. Metall. Mater. Sci. 44A (1), 224–234.
Jennett, N.M., Bushby, A.J., 2001. Adaptive Protocol for robust estimates of coatings properties by nanoindentation. In: Ozkan, C.S., Freund, L.B., Cammarata, B.C., Gao, H. (Eds.), Thin Films: Stresses and Mechanical Properties IX. MRS, Boston, pp. 73–78.
King, R.B., 1987. Elastic analysis of some punch problems for a layered medium. Int. J. Sol. Struct. 23 (12), 1657–1664.
Lebouvier, D., Gilormini, P., Felder, E., 1985. A kinematic solution for plane-strain indentation of a bilayer. J. Phys. D: Appl. Phys. 18, 199–210.
Liu, Y., Wang, B., Yoshino, M., Roy, S., Lu, H., Komanduri, R., 2005. Combined numerical simulation and nanoindentation for determining mechanical properties of single crystal copper at mesoscale. J. Mech. Phys. Sol. 53 (12), 2718–2741.
Martinez-Gonzalez, E., Ramirez, G., Romeu, J., Casellas, D., 2015. Damage induced by a spherical indentation test in tool steels detected by using acoustic emission technique. Exp. Mech. 55 (2), 449–458.
Panich, N., Sun, Y., 2004. Effect of penetration depth on indentation response of soft coatings on hard substrates: a finite element analysis. Surf. Coat. Technol. 182, 342–350.
Pelletier, H., 2006. Predictive model to estimate the stress-strain curves of bulk metals using nanoindentation. Tribol. Int. 39 (7), 593–606.
Pohl, F., Huth, S., Theisen, W., 2014. Indentation of self-similar indenters: an FEM-assisted energy-based analysis. J. Mech. Phys. Sol. 66, 32–41.
Saha, R., Nix, W.D., 2002. Effects of the substrate on the determination of thin film mechanical properties by nanoindentation. Acta Materialia 50 (1), 23–38.
Sun, Y., Bell, T., Zheng, S., 1995. Finite element analysis of the critical ratio of coating thickness to indentation depth for coating property measurements by nanoindentation. Thin Sol. Films 258 (1–2), 198–204.
Tricoteaux, A., Duarte, G., Chicot, D., Le Bourhis, E., Bemporad, E., Lesage, J., 2010. Depth-sensing indentation modeling for determination of elastic modulus of thin films. Mech. Mater. 42 (2), 166–174.
Tunvisut, K., O'Dowd, N.P., Busso, E.P., 2001. Use of scaling functions to determine mechanical properties of thin coatings from microindentation tests. Int. J. Sol. Struct. 38, 335–351.
Xu, H., Pharr, G.M., 2006. An improved relation for the effective elastic compliance of a film/substrate system during indentation by a flat cylindrical punch. Scripta Materialia 55, 315–318.
Xu, Z.H., Rowcliffe, D., 2004. Finite element analysis of substrate effects on indentation behaviour of thin films. Thin Sol. Films 447, 399–405.
Yonezu, A., Kuwahara, Y., Yoneda, K., Hirakata, H., Minoshima, K., 2009. Estimation of the anisotropic plastic property using single spherical indentation—an FEM study. Comput. Mater. Sci. 47, 611–619.